Open access Journal International Journal of Emerging Trends in Science and Technology
IC Value: 76.89 (Index Copernicus) Impact Factor: 4.219 **DOI:** https://dx.doi.org/10.18535/ijetst/v4i8.19

Geometrical and operational parameters effect on inline hole jet plate solar Air heater with longitudinal fins for cross and non-cross flow conditions

Authors
Mukesh Kumar Yadav[1], Rajen Kumar Nayak[2], [3]Manoj Kumar
[1]Research Scholar, Mechanical Engineering Department, BIT Sindri Dhanbad
[2]Assistant Professor, Mechanical Engineering Department, BIT Sindri Dhanbad
[3]Assistant Professor, Mechanical Engineering Department, BIT Sindri Dhanbad

Abstract
This paper is based on analytical study of flow and heat transfer in cross and non - cross flow inline hole jet plate solar air heater with fins attached underside the absorber surface. Results are presented for various fixed and variable geometrical and operational parameters such as jet hole diameter D = 6 - 10 cm, pitch of the holes X = 6 cm, number of jet holes, N = 480, height of the longitudinal fins L_f = 0.012m, pitch of the fins p = 3 mm, depth of the lower and upper channel, Z_1 and Z_2 = 8.0 cm, mass flow rates of air $\dot{m}_1$= 50 to 300 kg / hm^2 whereas $\dot{m}_2 = \dot{m}_1/2$for cross - flow and $\dot{m}_2 = 0$ for non - cross flow, solar intensity I_T = 650 W/m^2, wind velocity V_w = 1.3 m/s and ambient temperature T_A = 30^{o}C. The results show the T_o and h_{Pj} are higher in non - cross flow than cross flow condition whereas η_c is higher in cross - flow than non - cross flow than cross flow condition under same geometrical and operational parameters.
Keywords- Inline hole, Jet hole diameter, Collector efficiency, Heat transfer coefficient.

1. Introduction

The jet plate solar air heater is a non - conventional solar air heater which gives better performance than non - conventional solar air heater. By hitting on surface, the jet air breaks the surface thermal boundary layers of the absorber plate. As a result, the heat transfer coefficient between absorber plate and air pass have been increased in jet concept solar air heaters.

In earlier research works, the modifications are made on conventional solar air heaters by providing various shapes and design of artificial roughness on the absorber surface [1- 4]. The performance of flat plate solar air heater has also been enhanced by attaching the longitudinal fins over and underside the absorber plate [5, 6], double pass of air through the flow channel with fin attached [7] and one or more glass covers with the air flowing over and under the absorber surface [8 - 9]. Chaudhary et al. [10] analytically evaluated the gain in temperature increment and performance efficiency of the inline hole cross and non - cross flow jet concept air heater over that of the parallel plate air heater with duct depth 10.0 cm and length 2.0 m is 15.5^{o}C to 2.5^{o}C and 26.5% to 19.0 % respectively, for air flow rates in the range 50 to 250 kg/hm^2. The analytical investigations of effect of mass flow rate, depth of flow channel and length of collector on thermal performance and pressure drop through the channel with and without porous medium have been made by Adam et al. [11]. In a cross – flow inline hole jet plate solar air heater, the experimental and numerical results on heat transfer coefficient have been observed by Xing et al. [12]. R. Chauhan et al. [13] have been developed correlations for Nusselt number and friction factor in inline hole jet solar air heater.

The critical survey of literature shows that the very few works are available in the proposed area so the present analytical work is aim to focus on flow and heat transfer in inline hole jet plate solar air heater with longitudinal fins for cross and non-cross flow conditions.

1. Mathematical Formulation

The schematic diagram of the jet plate solar air heater is represented in Fig.1 which is having an air blower for supplying air through the channel, bottom plate, jet plate with inline hole (as shown in Fig. 2), black painted absorber plate with attached fins underside the absorber surface (α = 0.95), toughened glass cover plate (τ = 0.9), jet plate inserted between absorber and bottom plate, two flow channels, bottom and side insulation (σ = 0.034 W/m^{o}C) of thickness 5 cm and thermocouples imbedded to each plate. In cross - flow condition, mass flow rate of air ($\dot{m}_1$) between bottom plate and jet plate impinges out of the jet holes on the jet plate and mixes with $\dot{m}_2$ in the upper channel (as shown in Fig. 3) and subsequently the same comes out from the upper channel exit. Similarly for non - cross flow condition, since inlet of upper channel is closed so air ($\dot{m}_1$) from the bottom channel passes through the jet holes and strikes the lower surface of the absorber plate, finally air ($\dot{m}_1$) comes out from the upper channel exit as shown in Fig. 4. The supply air $\dot{m}_1$ and $\dot{m}_2$ may be controlled with the help of voltage regulated which is integrated with the air blower. Similarly, the absorber plate temperature (T_P), jet plate temperature (T_j) and bottom plate temperature (T_b) can be measured with the help of thermocouples which are embedded on the plates separately whereas the ambient temperature (T_A) and wind velocity (V_w) are recorded with the help of hot wire anemometer and solar intensity with the help of Pyranometer. The whole structure is supported on a movable steel frame.

For the present study, the details geometrical specifications of the set up are as length of air heater or fins L (2 m), width of air heater W (1 m), depth of lower and upper flow channel Z_1 and Z_2 (8 cm), holes in jet plate in inline jet plate N is 480, span-wise pitch of the jet holes X (6 cm), distance between absorber and cover d (2.54 cm), Pitch of the fins p (3 mm), height of the longitudinal fins L_f (0.012m), number of fins N_f is 20, thickness of fins δ_f (3 mm), thicness of absorber plate t (1 mm), thicness of jet plate t (4 mm), thicness of toughened glass cover t (4 mm) and thicness of insulation t (2.5 mm).

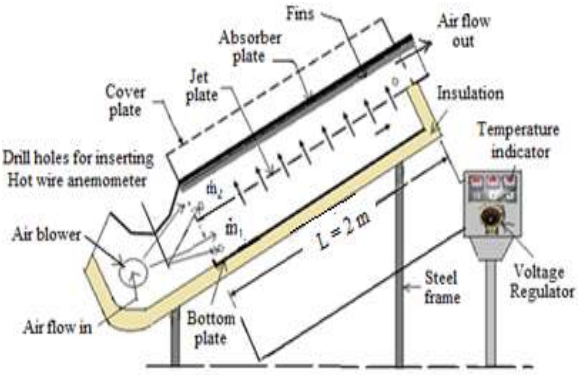

Fig. 1 Schematic diagram of the jet plate solar air heater with longitudinal fins attached underside the absorber surface along with elemental section of the absorber plate.

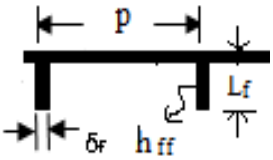

[Elemental section of the absorber plate]

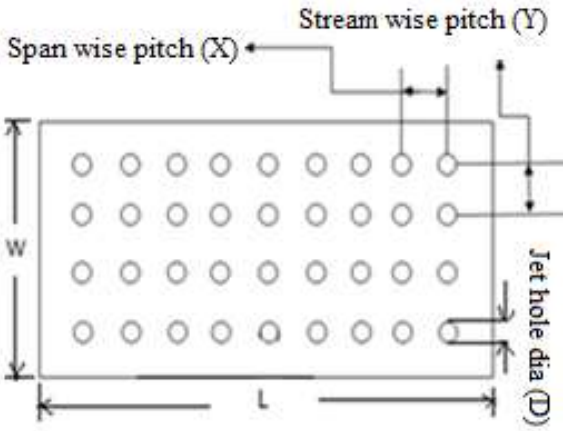

Fig. 2 Jet plate with inline hole

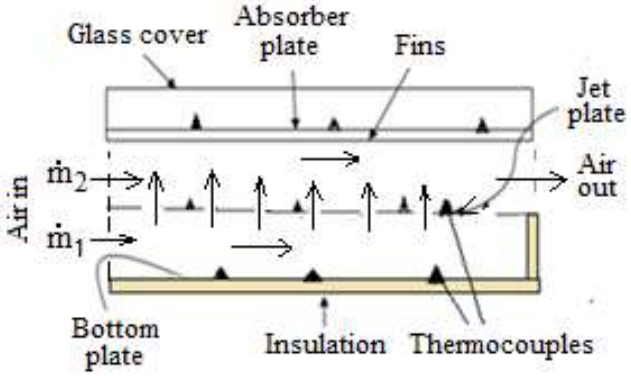

Fig. 3 Sectional view of cross - flow jet plate solar air heater with longitudinal fins underside the absorber surface

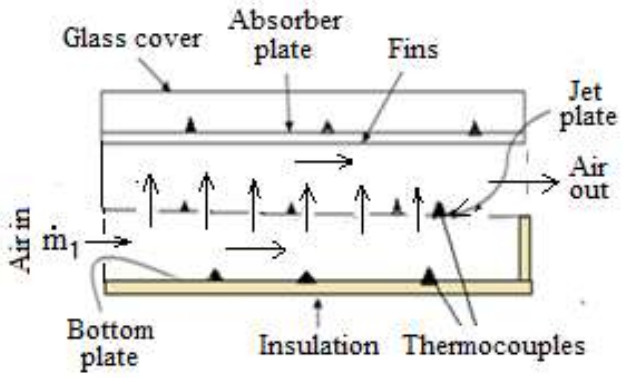

Fig. 4 Sectional view of non - cross flow jet plate solar air heater with longitudinal fins underside the absorber surface

The material for the jet plate is considered as aluminium alloy whereas the glass wool is considered for bottom and side insulation material. However, the measured operational likely wind velocity V_w (1.3 m/s), ambient temperature T_A (30°C) and solar intensity I_T (650 W/m^2) have been considered for finding the values of T_o, η_c and h_{Pj}.

2.1 Energy balance equation [10]:

For computing the performance of the air heater, the following equations are used under steady state condition,

$$h_{CS}(T_C - T_A) = h_{PC}(T_P - T_C) \quad (1)$$

$$I_T\tau\alpha = h_{PC}(T_P - T_C) + h_{cPa2}(T_P - T_{a2}) + \frac{2L_f \phi h_{ff}}{p}(T_P - T_{a2}) + h_{rpj}(T_P - T_j). \quad (2)$$

$$h_{rpj}(T_P - T_j) = h_{cja2}(T_j - T_{a2}) + h_{cja1}(T_j - T_{a1}) + h_{rjb}(T_j - T_b) \quad (3)$$

$$h_{rjb}(T_j - T_b) = h_{cba1}(T_b - T_{a1}) + U_b(T_b - T_A) \quad (4)$$

$$\dot{m}_1 C_P(T_{ol} - T_A) = h_{cja1}(T_j - T_{a1}) + h_{cba1}(T_b - T_{a1}) \quad (5)$$

$$\dot{m}_1 C_P(T_o - T_{ol}) + \dot{m}_2 C_P(T_o - T_A) = h_{cja2}(T_j - T_{a2}) + h_{cpa2}(T_P - T_{a2}) + \frac{2L_f \phi . h_{ff}}{p}(T_P - T_{a2}) \quad .....(6)$$

In equation (2) to (6),

$$T_{a1} = \frac{T_A + T_{ol}}{2} \text{ and } T_{a2} = \frac{T_i + T_o}{2}$$

where, $T_i = \frac{(\dot{m}_1 T_1 + \dot{m}_2 T_2)}{(\dot{m}_1 + \dot{m}_2)}$ is the inlet air temperature above jet plate in mixing of two flows of air $\dot{m}_1$ and $\dot{m}_2$ and $T_{a2} = \frac{(\dot{m}_1 T_1 + \dot{m}_2 T_2) + (\dot{m}_1 + \dot{m}_2)T_O}{2(\dot{m}_1 + \dot{m}_2)}$ is the air temperature at upper channel.

In addition, $h_{pa2,}$ the coefficient of heat transfer from absorber plate to the air above the jet plate, is given by

$$h_{pa2} = h_{Pj}\frac{(T_P - T_{ol})}{(T_P - T_{a2})} \quad (7)$$

The average efficiency of the system may be then obtained by using the standard correlation:

$$\eta_c = \frac{(\dot{m}_1 + \dot{m}_2)C_p(T_O - T_A)}{I_T A} \quad (8)$$

2.2 Heat Transfer Coefficients [10]

The convective heat transfer coefficient, h_w, for air flowing over the outer surface of the glass cover depends on wind velocity V_w[14]. Thus, the obtained results are:

$$h_{CS} = h_w + h_{rCS} \quad (9)$$

Where,

$$h_w = 5.7 + 3.8V_w \quad (10)$$

$$h_{rCS} = \varepsilon_C \sigma(T_C^4 - T_S^4)(T_C - T_S) \quad (11)$$

Where,

$$T_S = 0.0552(T_A)^{1.5} \quad (12)$$

The coefficient of heat transfer, h_{PC} from absorber to the cover plate is obtained from,

$$h_{PC} = h_{cPC} + h_{rPC} \quad (13)$$

where, the convective heat transfer coefficient between absorber plate to cover,

$$h_{cPC} = Nu_c \frac{k_a}{d} \quad (14)$$

$$Nu_c = 0.093(Gr_c)^{0.31} \quad (15)$$

$$Gr_c = \frac{g\beta(T_P - T_{C)}}{\nu} \quad (16)$$

The radiative heat transfer between absorber plate to cover,

$$h_{rPC} = \frac{\sigma(T_P^2 + T_C^2)(T_P + T_C)}{\frac{1}{\varepsilon_P} + \frac{1}{\varepsilon_C} - 1} \quad (17)$$

The average plate- to- jet air heat transfer coefficients [10] are;

$$h_{Pj} = Nu_{Pj} \frac{k_a}{d} \quad (18)$$

With,

$$N_{Pj} = F_1 F_2 (\mathrm{Re}_D)^m (Z_1 / D)^{0.091} \quad (19)$$

The jet Reynolds number,

$$\mathrm{Re}_D = \frac{\rho V_j D}{\mu} \quad (20)$$

where, jet air velocity, $V_j = \frac{4\dot{m}_1}{\rho N \pi D^2}$

For, $1 \le Z_1/D \le 5$, $300 \le \mathrm{Re}_D \le 3 \times 10^4$

The parameters m, F_1, F_2 are evaluated for $300 \le \mathrm{Re}_D \le 3000$. In case of non - cross flow ($\dot{m}_2 = 0$) is considered as $F_2 = 1$, which decreases with an increasing cross flow velocity. The forced convective coefficients for heat transfer from jet plate to air above (h_{cja2}) be as,

$$h_{cja2} = \frac{A_e}{A} Nu_{ja2} \frac{k_a}{D_2} \quad (21)$$

where,

$$Nu_{ja2} = 0.0293(\mathrm{Re}_{ja2})^{0.8},$$

$$\mathrm{Re}_{ja2} = \frac{(\dot{m}_1 + \dot{m}_2) L D_2}{Z_2 \mu} \quad \text{and}$$

$$A_e = A - N\pi D^2 + 2N_1 / N$$

The radiative heat transfer coefficient between the absorber and jet plate be as,

$$h_{rPj} = \frac{\sigma(T_P^2 + T_j^2)(T_P + T_j)}{\frac{1}{\varepsilon_p} + \frac{1}{\varepsilon_j} - 1} \quad (22)$$

Similarly, the radiative heat transfer coefficient between jet plate and back plate is:

$$h_{rjb} = \frac{\sigma(T_j^2 + T_b^2)(T_j + T_b)}{\frac{1}{\varepsilon_j} + \frac{1}{\varepsilon_b} - 1} \quad (23)$$

The bottom loss heat coefficient is calculated by using,

$$U_b = \frac{k_i}{l} \quad (24)$$

The friction factor for a rectangular smooth duct calculated from modified Blassius equation as,

$$f_S = 0.085(\mathrm{Re}_{ja2})^{-0.25} \quad (25)$$

2. **Result And Discussion**

3.1 *Variation of outlet air temperature (T_o) and collector efficiency (η_c) with jet hole diameter (D) and mass flow rates of air, ($\dot{m}_1$ and $\dot{m}_2$)*

The effect of jet hole diameter (D) and mass flow rates of air ($\dot{m}_1$ and $\dot{m}_2$) on the outlet air temperature (T_o) and collector efficiency (η_c) are presented in Figs. 5 and 6 respectively. The examination of the curves reveal that both T_o and η_c decreases with increase in jet hole diameter (D) and mass flow rates of air ($\dot{m}_1$ and $\dot{m}_2$) through the channel for both cross and non – cross flow conditions. The highest values of T_o and η_c are obtained at lowest jet plate hole diameter (D) because of getting higher jet air velocity (V_j). The similar result has been shown in the literature of Chaudhury et al [10]. For fixed mass flow rates ($\dot{m}_1$ and $\dot{m}_2$) and jet hole diameter (D), the outlet air temperature(T_o) is found higher in case of non - cross flow whereas the collector efficiency (η_c) is obtained higher in case of cross - flow inline hole jet plate solar air heater with longitudinal fins. For fixed $\dot{m}_1$ (50 kg / hm^2) and D (6 mm), the gain in outlet air temperature (T_o) is found 13.4% higher in non - cross flow as compared to cross - flow condition whereas the collector efficiency (η_c) is obtained 8.2% higher in cross -

flow with respect to non - cross flow condition for $\dot{m}_1$ (50kg/hm^2) and D (6 mm). The higher collector efficiency in case of cross - flow is due to the mixing of two flows of air ($\dot{m}_1$ and $\dot{m}_2$) in the upper channel of the air heater.

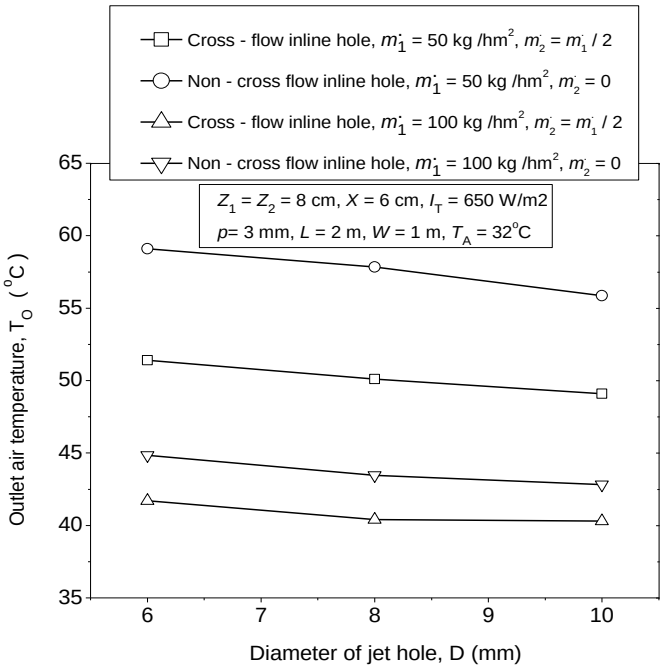

Fig. 5 Variation of outlet air temperature (T_o) with jet hole diameter, D (6 mm – 10 mm) and mass flow rates of air, $\dot{m}_1$ and $\dot{m}_2$

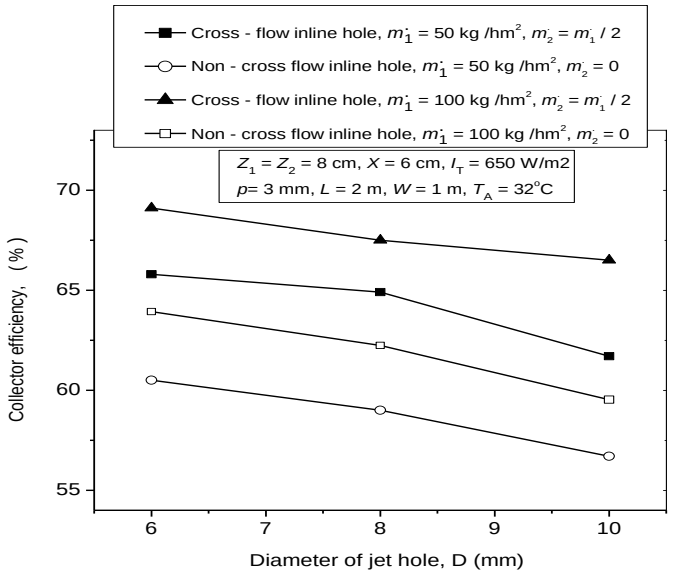

Fig. 6 Variation of collector efficiency (η_c) with jet hole diameter, D (6 mm - 10 mm) and mass flow rates of air, $\dot{m}_1$ and $\dot{m}_2$

3.2 *Effect of jet hole diameter (D) and mass flow rates of air, ($\dot{m}_1$ and $\dot{m}_2$) on absorber plate to jet air heat transfer coefficient (h_{Pj})*

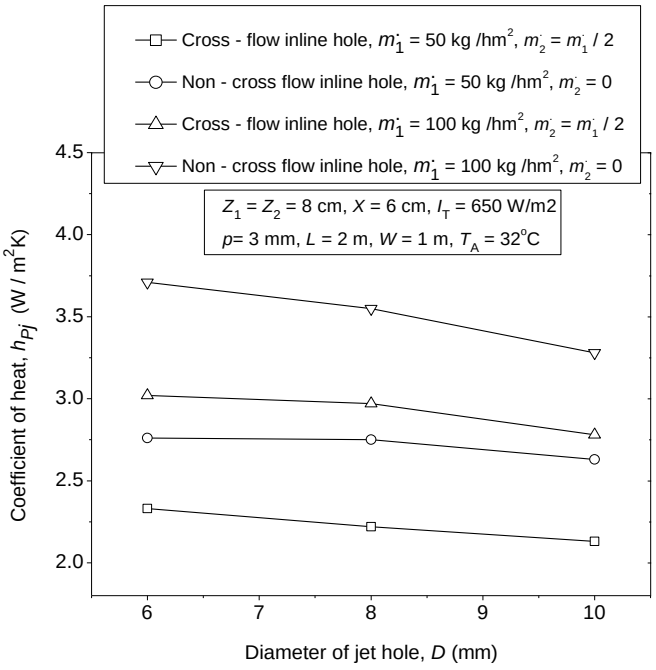

Fig. 7 Variation of heat transfer coefficient (h_{Pj}) with jet hole diameter,D (6 mm – 10 mm) and mass flow rates of air, $\dot{m}_1$ and $\dot{m}_2$

The effect of jet hole diameter (D)and mass flow rates of air,($\dot{m}_1$ *and* $\dot{m}_2$)on the absorber plate - to - jet air heat transfer coefficient (h_{Pj}) is shown in Fig. 7. Under both cross and non - cross flow cases, the heat transfer coefficient (h_{Pj})increases with increase in mass flow rates of air,($\dot{m}_1$ *and* $\dot{m}_2$)whereas the heat transfer coefficient (h_{Pj}) decreases with increase in jet hole diameter (D) for same geometrical and operational parameters in the analysis. This highest value of h_{Pj} is obtained at lowest jet plate hole diameter, D (6 mm) and higher mass flow rates of air,$\dot{m}_1$ (100 kg / hm^2)due to of higher jet air velocity (V_j). For fixed mass flow rate ($\dot{m}_1$) and jet hole diameter (D), the heat transfer coefficient (h_{Pj}) is found higher in non - cross inline hole with respect to cross - flow inline hole jet plate solar air heater with longitudinal fins. For fixed $\dot{m}_1$ (50 kg/hm^2) and jet hole diameter D (6 mm), the heat transfer coefficient (h_{Pj})is found 18.45% higher in non - cross flow that cross flow condition whereas the heat transfer coefficient (h_{Pj})is obtained 22.85% higher in non - cross flow that cross flow condition for $\dot{m}_1$ (100 kg/hm^2) and jet hole diameter D (6 mm).

3.3 Variation of friction factor (f_s) with flow Reynolds number (Re_{ja2})

For $\dot{m}_1$ (50 - 300 kg /hm^2) and D (6 mm - 10 mm), the variation of friction factor (f_s) is a function of flow Reynolds number (Re_{ja2}) under cross and non - cross flow inline hole jet plate solar air heater is

shown in Fig. 8. Under both the cases, curves indicate that friction factor (f_s) decreases with increase in flow Reynolds number. For all range of $\dot{m}_1$ (50 - 300 kg / hm^2) and Re_{ja2} (2500 – 18000), the friction factor (f_s) is found higher in non - cross flow than cross - flow condition which also complies the above results for higher T_o and h_{Pj} in non - cross flow inline hole jet plate solar air heater with longitudinal fins attached underside the absorber surface.

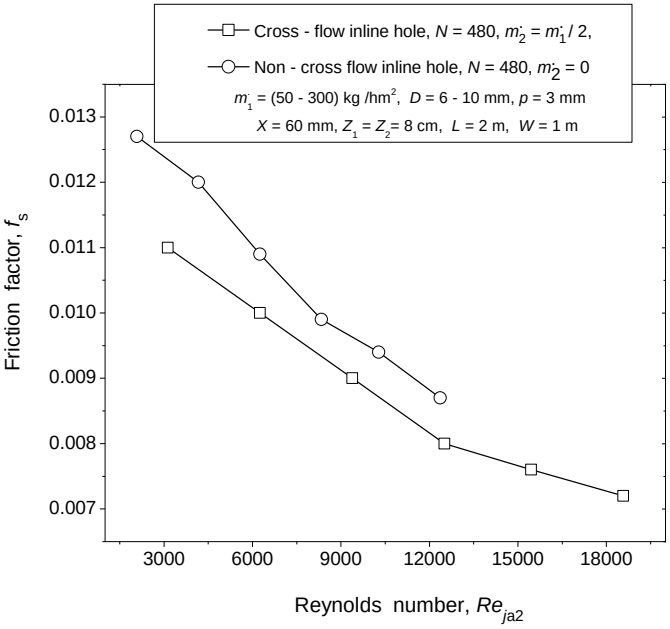

Fig.8 variation of friction factor (f_s) with Reynolds number (Re_{ja2})

Nomenclature

A Surface area of the absorber plate, m^2
A_e Effective heat transfer area of jet plate, m^2
Cp Specific heat capacity of air, Wh/kg˚C
d Distance between absorber plate and cover, m
D Diameter of the jet hole, m
D_1 Hydraulic diameter of the bottom channel, m $D_1 = 4WZ_1/2(W+Z_1)$
D_2 Hydraulic diameter of the upper channel, m $D_2 = 4(pZ_2 - \delta_f)/ 2(p + L_f)$
f_s Friction factor
F_1 Dimensionless constant
F_2 Cross - flow degradation factor
g Acceleration due to gravity, m/s^2
G_1 Mass flow velocity of air impinging out of holes, kg/hm^2
G_2 Mass flow velocity of cross flow air, kg/hm^2
G_r Grashoff number
h_{CS} Heat transfer coefficient from cover plate to surrounding air, W/m^{2}K
h_{ff} Heat transfer coefficient between the fin surface and air stream, W /m^{2}K
h_{PC} Heat transfer coefficient between from absorber to the cover plate, W/m^{2}K
h_{cPC} Convective heat transfer coefficient between absorber plate to cover plate,W/m^{2}K
h_{cja1} Convective heat transfer coefficient from jet plate to lower channel air, W/m^{2}K
h_{cja2} Convective heat transfer coefficient from jet plate to upper channel air, W/m^{2}K
h_{cba1} Convective heat transfer coefficient from bottom plate to lower channel air, W/m^{2}K
h_{rcs} Radiative heat transfer coefficient from cover plate to surrounding air, W/m^{2}K
h_{rjb} Radiative heat transfer coefficient between jet plate and bottom plate, W/m^{2}K
h_w Coefficient of wind related heat transfer, W/ m^{2}K
h_{rpj} Radiative heat transfer coefficient between absorber and jet plate, W/m^{2}K
h_{Pa2} Coefficient of heat transfer from absorber plate to upper channel air, W/m^{2}K
h_{Pj} Average plate-to-jet air heat transfer coefficient, W/m^{2}K
hc_{Pa2} Convective heat transfer coefficient from absorber plate to upper channel air, W/m^{2}K
I_T Incident solar intensity, W/m^2
k_a Thermal conductivity of air flowing through duct, W/mk
l_i Glass wool thickness, m
L Length of air heater, m
L_f Height of the longitudinal fins, m
$\dot{m}_1$ Mass flow rate of air in parallel plate and bottom channel, kg/s
$\dot{m}_2$ Mass flow rate of of air in cross - flow, kg/s
N Total number of jet holes in jet plate
Nu_{Pj} Nusselt number between absorber and jet plate
p Pitch of the fins, m
Re_{ja2} Flow Reynolds number between absorber and jet plate
T_A Ambient temperature, ^{o}C
T_1 Inlet temperature of air at bottom channel, ^{o}C
T_2 Inlet temperature of air at upper channel, ^{o}C
T_a Channel air temperature in parallel plate air heater, ^{o}C
T_{a1} Air temperature at lower channel, ^{o}C
T_{a2} Air temperature at upper channel, ^{o}C
T_i Inlet air temperature above jet plate in mixing of air,
T_j Jet plate temperature, ^{o}C
T_o Outlet air temperature, ^{o}C

T_{ol} Outlet air temperature at jet hole, ^oC
T_P Absorber plate temperature, ^oC
V_w Wind velocity, m/s
W Air heater width, m
X Stream wise pitch of the holes, m
Y Span wise pitch of the holes, m
Z Total depth of solar air heater (Z_1+Z_2), m
Z_1 Spacing between jet and bottom plate, m
Z_2 Spacing between jet and absorber plate, m

Greek Symbols

α Solar absrptivity of absorber plate
τ Reflectivity of glass cover plate
β Coefficient of thermal expansion, K^{-1}
ϕ Effectiveness of fins
σ Stefan Boltzman constant, $W / m^2 k^4$
η_c Collector efficiency
ρ Density of air, kg / m^3
μ dynamic viscosity of air, Pa.sec
ν kinematic viscosity of air, m / s^2
δ_f Thickness of fins
ε_R thermal emittance of surface R

Subscripts

a air flowing through collector
b bottom plate
C cover plate
i inlet air at upper channel
j jet air / jet plate
o outlet air at heater exit
ol outlet air at jet hole
P absorber plate
S sky
t thickness

Conclusions

In the present study, it is concluded that the outlet air temperature (T_o) and heat transfer coefficient (h_{Pj}) are higher in non - cross flow than cross - flow condition for fixed jet hole diameter, *D* (6 mm) and mass flow rate ($\dot{m}_1$and $\dot{m}_2$). However, the collector efficiency (η_c) is obtained higher in case of cross - flow inline hole jet plate solar air heater with longitudinal fins. For fixed $\dot{m}_1$ (50 kg/hm^2) and jet hole diameter *D* (6 mm), the heat transfer coefficient (h_{Pj})is found 18.45% higher in non - cross flow that cross flow condition whereas the heat transfer coefficient (h_{Pj})is obtained 22.85% higher in non - cross flow that cross flow condition for $\dot{m}_1$ (100 kg/hm^2) and jet hole diameter *D* (6 mm). The higher value of friction factor in case of non - cross flow complies the higher gain increment of outlet air temperature (T_o) and heat transfer coefficient (h_{Pj}) in non - cross flow than cross - flow inline hole jet plate solar air heater with longitudinal fins for same geometrical and operational parameters

References

[1] E. K Akpinar , F Kocyigit, Experimental invesestigation of thermal performance of solar air heater having different obstacles on absorber plates, Int common Heat Mass 37 (4) (2010) 416-421.

[2] B S Romdhane, The air solar collectors: Comparative study, introduction of baffles to favor the heat transfer, Solar Energy 81 (1) (2007) 139-149. doi: 10.1016 / j.solener.2006.05.002.

[3] M K Seluk, Solar air heaters and their applications, Academic Press, New York,1977.

[4] W Gao, W Lin , T Liu , C Xia C, Analytical and experimental studies on the thermal performance of cross - corrugated and flat – plate solar air heater, Applied Energy 84 (4) (2007) 623-637.

[5] Thombre, Sukhatme, 1995 Turbulent Flow and Friction Factor Characteristics of Shrouded Fin Arrays with Uninterrupted Fins, Experimental Thermal and Fluid Sc. 10,338, 1991.

[6] S N Singh, Performance Studies on Continuous Longitudinal Fins Solar Air Heater, Journal of ISM Dhanbad, vol. 2, 2006.

[7] A Omojaro, L Aldabbagh , Experimental performance single and double pass solar air heater with fins and steel wire mesh as absorber, Applied Energy 87 (12) (2010) 3759-3765. doi:10.1016 /j. Apenergy. 2010.06. 020.

[8] C H Liu, Sparrow E. M, Convective radiative interaction a parallel plate channel - application to air operated solar collectors, Int. J. Heat Mass Transfer. 23 (8) (1980) 1137-1146.

[9] H M Tan, Charters W. W. S, Experimental investigation of forced - convective heat transfer for fully developed turbulent flow in a rectangular duct with asymmetric heating, Solar Energy 13(1) (1970) 121-125.

[10] C Chaudhary, H P Garg, Evaluation of a Jet Plate Solar Air Heater, Solar Energy, 46

[11] N M Adam, BAA Yousef, Performance Analysis for Flat Plate Collector with and Without Porous Media, Journal of Energy in Southern Africa, Volume 19 No 4, 2008

[12] X Yunfei, S Sebastian, W Bemhard, Experimental and Numerical Investigation of Heat Transfer Characteristics of Inline and Staggered Arrays of Impinging Jets, J. *Heat Transfer*132(9), 2010.

[13] Chauhan, Ranchan., Thakur, N S., Heat transfer and friction factor correlation for jet impingement jet solar air heater, Experimental Thermal and Fluid Science 44 (2013) 760

[14] W. A. McAdams, Heat Transmission, 3rd edition, McGraw-Hill, New York, p-249 (1954)